Abundances and significance of platinum group elements in carbonatites from China

7 authors, including:

Cheng Xu
Nanjing University of Science and Technology
62 PUBLICATIONS 569 CITATIONS

SEE PROFILE

Liang Qi
Chengdu University of Technology
111 PUBLICATIONS 2,855 CITATIONS

SEE PROFILE

Yan-Jing Chen
Peking University
309 PUBLICATIONS 7,129 CITATIONS

SEE PROFILE

Some of the authors of this publication are also working on these related projects:

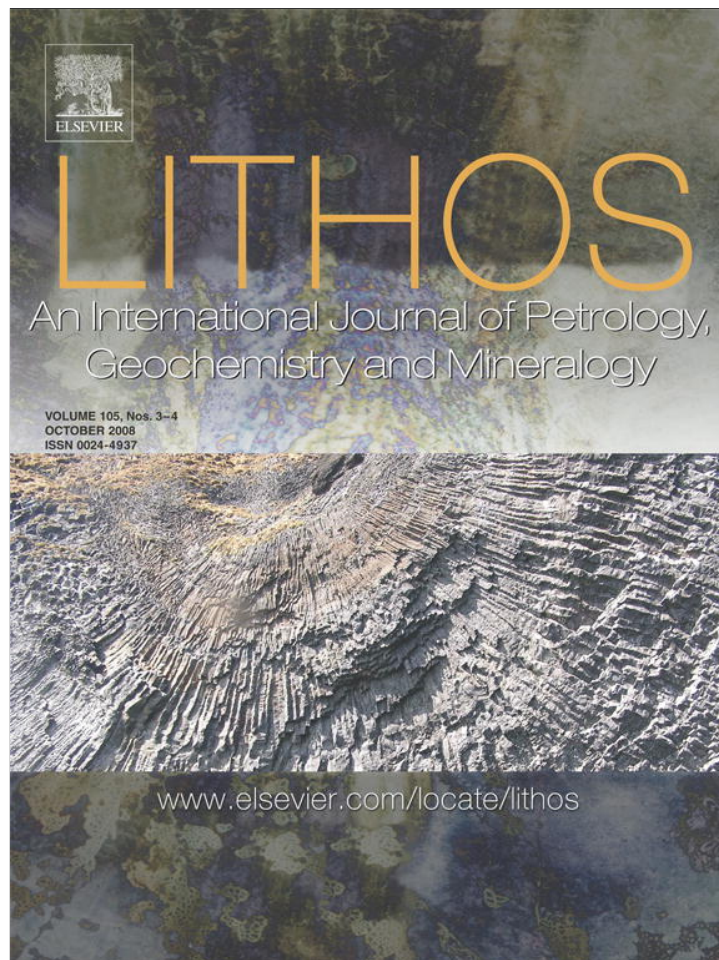Project Great Oxidation Event and Precambrian mineral deposits View project

Project magmatic hydrothermal deposits View project

ELSEVIER

LITHOS

An International Journal of Petrology,
Geochemistry and Mineralogy

VOLUME 105, Nos. 3–4
OCTOBER 2008
ISSN 0024-4937

www.elsevier.com/locate/lithos

Abundances and significance of platinum group elements in carbonatites from China

Cheng Xu [a,*], Liang Qi [a], Zhilong Huang [a], Yanjing Chen [b], Xuehui Yu [c], Linjun Wang [a], Endong Li [c]

[a] Laboratory of Materials of the Earth's Interior and Geofluid Processes, Institute of Geochemistry, Chinese Academy of Sciences, Guiyang 550002, China
[b] Department of Geology, Peking University, Beijing 100871, China
[c] Department of Geology, China University of Geosciences, Beijing 100083, China

ARTICLE INFO

ABSTRACT

The concentrations of the platinum group elements (PGEs: Ir, Ru, Rh, Pt, Pd) were determined in 29 extrusive and intrusive carbonatites from 7 locations in China. The samples were analyzed using an improved Carius tube with high temperature and high pressure. All samples are characterized by low total PGE contents (0.07–2.5 ppb), and only trace magmatic sulfides are observed in thin sections. The carbonatites may reach sulfur saturation because they are known to be derived by small degrees of partial melting (<1%). The PGEs may be compatible in sulfides with very high sulfide–carbonatite melt partition coefficients. Segregation of an immiscible sulfide melt can result in the loss of PGEs in the carbonatites. Compared with the intrusive and silicate-poor extrusive carbonatites, the silicate-rich extrusive carbonatite contains relatively abundant clinopyroxene and titanomagnetite and higher IPGE (Ir and Ru) contents. This implies that IPGEs may be compatible in these mineral phases. The low IPGE abundances and fractionated patterns in the intrusive and silicate-poor extrusive carbonatites reflect that they may have experienced significant fractionation of sulfides and IPGE-rich mafic silicates and oxides before final emplacement. The high PGE compositions in the silicate-rich extrusive carbonatite may represent mantle materials entrained by the rising carbonatite magma.

© 2008 Elsevier B.V. All rights reserved.

1 . Introduction

Carbonatites are magmatic, carbonate-rich rocks derived from the mantle (Bell and Blenkinsop, 1987; Keller and Hoefs, 1995). They have been found on all the continents except Antarctica and two oceanic localities (e.g. Bell, 1989), and contain valuable information about the nature of the mantle (e.g. Bell and Tilton, 2001; Hoernle et al., 2002; Tappe et al., 2007). However, a major question concerning carbonatite petrogenesis is whether or not the compositions of the rocks represent those of the parental magmas (e.g. Ionov and Harmer, 2002; Woolley and Church, 2005; Xu et al., 2007). Most intrusive carbonatites have aureoles of alkali metasomatized country rocks, reflecting the loss of alkalis and probably other elements. Bailey (1993) and Woolley and Church (2005) suggested that extrusive carbonatites were essential for understanding the wider aspects of cabonatite magmatism. Intrusive and extrusive carbonatites reflect not only the physical differences of their emplacement, but also possibly compositional differences. Due to their highly siderophile and chalcophile nature, platinum group element (PGE) systematics have the potential to provide key information about mantle processes, such as partial melting, melt percolation and mantle metasomatism (e.g.

Büchl et al., 2002; Momme et al., 2006; Ionov et al., 2006). However, the geochemical behavior of PGEs in the mantle is not well-understood because of the limited availability of PGE data on mantle-derived rocks. Thus, comparison of PGEs in intrusive and extrusive carbonatites may provide new information on petrogenesis of carbonatites and geochemical behavior of PGEs in the mantle source.

Carbonatites may contain platinum group minerals. For example, Rudashevsky et al. (2001) identified isoferroplatinum, cooperite, sperrylite, mertieite in the carbonatites from Phalaborwa and Kovdor, Russia. However, reports of PGE abundances of carbonatites are sparse. Although Xu et al. (2003b) determined PGE contents of carbonatites from Maoniuping, Southwest China, the technique they used involved the digestion by sodium peroxide fusion and may not be suitable for PGE-poor carbonatites. To obtain reliable PGE data, the PGE contents of representative carbonatites from China were determined using our newly developed dissolution technique. The dissolution technique utilizes *aqua regia* to digest 10 g of sample in an improved Carius tube at a temperature of 300 °C (Qi et al., 2007). In this paper, we report new PGE data and discuss the behavior of the PGEs during the formation and evolution of carbonatites.

2. Samples

Twenty nine carbonatite samples were collected from Daluxiang (DLX), Maoniuping (MNP) in Sichuan Province, Miaoya (MY), Shaxiongdong (SXD) in Hubei Province, Huayangchuan (HYC),

* Corresponding author. Institute of Geochemistry, Chinese Academy of Sciences, 46 Guanshui Road, Guiyang 550002, Guizhou Province, China. Tel.: +86 851 5895194; fax: +86 851 5891117.
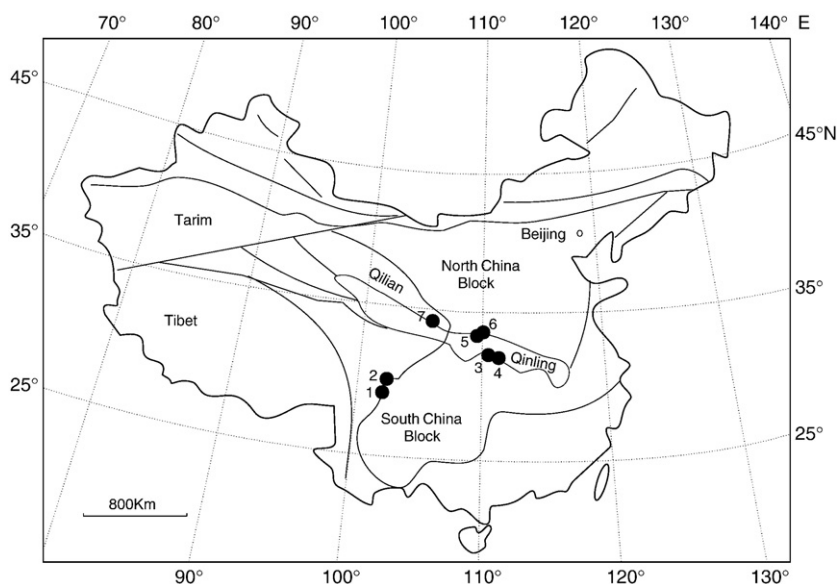E-mail address: xucheng1999@hotmail.com (C. Xu).

Fig. 1. Sample locations in China. 1, Daluxiang; 2, Maoniuping; 3, Miaoya; 4, Shaxiongdong; 5, Huayangchuan; 6, Huanglongpu; 7, Lixian.

Huanglongpu (HLP) in Shanxi Province, Lixian (LX) in Gansu Province (Fig. 1) for PGE analyses. The DLX and MNP carbonatites are associated with syenites and emplaced in the western margin of the South China block. Unlike most known carbonatites within plates generated by anorogenic processes (e.g. rifting), they occur in a continental collision zone, formed by the Indo–Asian continental collision since the Paleocene period (ca. 65–45 Ma; Yin and Harrison, 2000; Xu et al., 2003a; Hou et al., 2006). The MY and SXD carbonatites are situated in the northern margin of the South China block. Xu et al. (in press) obtained the zircon U–Pb age of 441.8 Ma from the SXD syenites associated with carbonatites and suggested that they formed in a rifting environment. The HYC and HLP carbonatites occur in the southern margin of the North China block. K–Ar dating of phlogopite and Re–Os on molybdenite gave ages of 181 Ma (Yu, 1992) and 221 Ma (Huang et al., 1994), respectively. These carbonatites formed in a complex tectonic environment, which may be related with the Triassic collision between the South and North China blocks along the Qinling (e.g. Meng and Zhang, 2000).

The LX carbonatites are located at the contact between the Qinling and Qilian orogenic belts. The rocks are volcanic and associated with Cenozoic kamafugites (Yu et al., 2003, 2006). They consist of pyroclasitcs and lava. Presently, there are only 49 known extrusive carbonatite occurrences (Woolley and Church, 2005).

Brief descriptions and modal abundances for all of the samples used in this study are given in Table 1. They are calciocarbonatites and composed dominantly of calcite. The sample LX-2 contains relatively abundant mantle materials of lapilli and clinopyroxene. The lapilli are spherical and essentially consist of randomly distributed microlites of clinopyroxene, titanomagnetite, apatite, melilite and calcite in a volcanic glass groundmass.

Table 1
Carbonatite samples in this study: modal abundances, nature, associated silicate rocks and ages

Sample	Modal abundances	Nature of occurrence	Associated silicate rocks	Ages
Daluxiang	80–90% calcite, 2–5% alkali feldspar, 2–4% quartz, 1–3% arfvedsonite, 1–3% celestite, 1–2% fluorite, ~1% REE minerals, 0–1% aegirine, <1% apatite, <1% sulfides	Dyke	Syenite	–
Maoniuping	92–95% calcite, 1–2% alkali feldspar, 1–2% arfvedsonite, 1–2% aegirine, 1–2% biotite, <1% apatite, <1% REE minerals	Sill	Syenite	31.7±0.7 Ma K–Ar dating on arfvedsonite
Miaoya	80–95% calcite, 1–8% biotite, 1–3% alkali feldspar, 1–3% sulfides, 0–2% quartz, 1–2% REE minerals, 0–1% graphite, <1% apatite	Stock	Syenite	–
Shaxiongdong	80–90% calcite, 2–6% alkali feldspar, 3–5% biotite, 3–5% aegirine, 1–2% REE minerals, <1% apatite, <1% pyrochlore, <1% magnetite and sulfides	Dyke	Syenite	441.8±2.2 Ma U–Pb dating on zircon from associated syenite
Huayangchuan	92–95% calcite, 1–2% alkali feldspar, 0–1% quartz, 0–1% celestite, 0–1% barite, 0–1% phlogopite, <1% arfvedsonite, <1% aegirine, <1% apatite, <1% magnetite and sulfides	Dyke	Syenite	181 Ma K–Ar dating on phlogopite
Huanglongpu	92–96% calcite, 1–2% alkali feldspar, 0–2% quartz, 0–1% celestite, <1% phlogopite, <1% apatite, <1% molybdenite, <1% magnetite and sulfides	Dyke	Syenite	221 Ma Re–Os dating on molybdenite
LX (Lixian)-1	95% calcite, 2% phlogopite, 1% clinopyroxene, 1% nepheline, 1% apatite and titanomagnetite	Lava, pyroclastics	Kamafugite	22–23 Ma Ar–Ar dating on phlogopite from associated kamafugite
LX (Lixian)-2	74% calcite, 20% lapilli, 2% clinopyroxene, 1% melilite, 1% phlogopite,1% nepheline, 1% apatite and titanomagnetite			

The modal abundances are estimated by point counting and backscattered electron images. References for ages are from Yu (1992), Huang et al. (1994), Pu (2001), Yu et al. (2006) and Xu et al. (in press). Notably, abundant microlites of clinopyroxene and titanomagnetite occur in the lapilli of sample Lixian-2.

3. Analytical methods

The PGE concentrations were determined on a VG Plasma-Quad Excell ICP-MS at the University of Hong Kong. The conventional Carius tube method for PGE analysis yields total procedural blanks as low as 0.04 ng for Pt and 0.005 ng for other PGEs, but uses small amounts (usually 1–2 g) of sample (Meisel et al., 2003). To increase the sample mass and reduce the nugget effects, an improved Carius tube method was used in this study. The HCl and HNO_3 were purified by sub-boiling distillation. Water was obtained from 18 MΩ cm grade Millipore purification system. Spike solutions with enriched stable isotopes ^{101}Ru, ^{105}Pd, ^{193}Ir, and ^{194}Pt were prepared from pure metals (US Services Inc., Oxbow, N.J.). An ICP multi-element standard solution of 100 μg/ml Pt, Pd, Rh, Ru and Ir (AccuStandard, USA) was used and diluted as required for calibration of the spike and mono-isotope element Rh. For pre-concentration of PGEs by Te co-precipitation, the Te solution (2 mg/ml) was prepared by dissolving 0.5 g of TeO_2 in 10 ml of concentrated HCl and diluted to 200 ml with distilled water. The $SnCl_2$ solution (20%, w/v) was prepared by dissolving 50 g of $SnCl_2$ in 250 ml of 6 M HCl, and then purified by Te-coprecipitation method (Qi et al., 2004). The Carius tube used in this study is a conventional 75 ml borosilicate glass tube similar to those described by Shirey and Walker (1995). They were filled with 60% *aqua regia* and heated to about 80 °C and 5 h for cleaning. The high pressure autoclave was made of stainless steel with inner length of 280 mm and diameter of 28 mm (Fig. 2).

For analysis, 10 g of sample was weighed into 125 ml Savillex Teflon beaker and mixed with spike solution. After decarbonating of the sample with about 20 ml of 10 M HCl, the sample was evaporated to dryness and transferred to a Carius tube for further digestion with 10 ml of 12 M HCl and 6 ml of 16 M HNO_3. The sealed Carius tube was placed in the high pressure autoclave, which was then filled with about 55 ml water. The external pressure produced by water balanced the internal pressure of the Carius tube to keep it from exploding. The autoclave was sealed and heated to 300 °C in an electric oven for about 15 h. After slowly cooling in air to room temperature, the Carius tube was opened, and the solution was transferred into a 50 ml centrifuge tube and then rinsed with about 15 ml water. The tube was
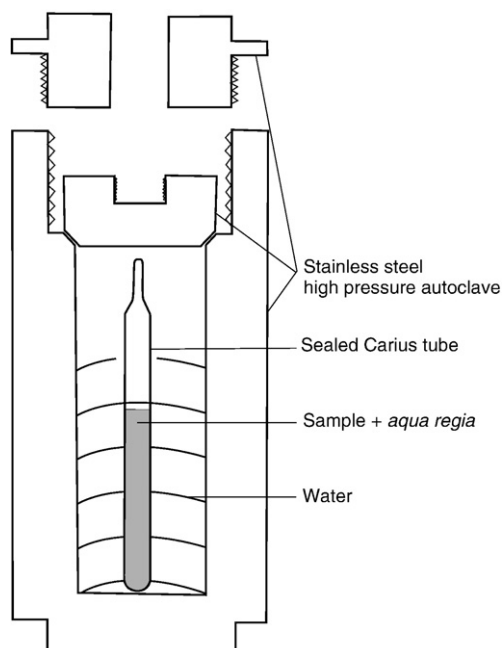

Fig. 2. Experimental configuration.

Table 2
Platinum group element abundances (ppb) in the analytical blank

Samples	1	2	3	4	5
Ir	0.002	0.003	0.003	0.002	0.002
Ru	0.002	0.001	0.002	0.002	0.003
Rh	0.003	0.002	0.002	0.002	0.002
Pt	0.025	0.023	0.019	0.018	0.024
Pd	0.033	0.036	0.040	0.031	0.039

centrifuged at 2200 rpm for 6 min. The centrifuged solution was transferred back into the beaker, dried down and reconverted into the chloride form by HCl. The residue was dissolved by 40 ml of 2 M HCl and used for preconcentrating PGEs by Te-coprecipitation. After this step, a Dowex 50 WX 8 cation exchange resin and a P507 extraction chromatograph resin combined in the same column were used to remove all the main interfering elements, including Cu, Ni, Zr and Hf (Qi et al., 2004). The final solution obtained from the exchange procedure was evaporated to 2 ml and made up to 5 ml for ICP-MS measurement. The Pt, Pd, Ru and Ir were determined by isotope dilution. For Rh a ^{194}Pt spike was used as an internal standard as described by Qi et al. (2004). Total procedure blanks are listed in Table 2. Additional information on accuracy and precision can be found in Qi et al. (2007).

Whole rock Ni and Cu were analyzed by solution ICP-MS at the University of Hong Kong. Details are given in Liang et al. (2000). Replicate analyses and results from standards indicated that the accuracy of the element determinations was better than 10%.

4. Results

Concentrations of PGEs in the carbonatites are listed in Table 3 and are normalized using the primary mantle values (Fig. 3).

The carbonatites have low total PGE concentrations ranging from 0.07 ppb to 2.5 ppb. They have mantle-normalized patterns with positive slopes enriched in Pd relative to Ir (Fig. 3). The intrusive carbonatites have lower Ni, Cu and Ir contents relative to the extrusive ones. Some DLX and MNP samples display $(Pt/Pd)_n$ ratios >1, and MY and SXD show relatively low $(Pt/Ir)_n$ ratios. However, none of the samples show obvious differences in PGE absolute or relative abundances, although these intrusive carbonatites were emplaced in different tectonic settings and have different ages and isotopic compositions (e.g. initial $^{87}Sr/^{86}Sr$ ratios for DLX, MNP, MY, SXD, HYC, HLP are 0.7078–0.7080, 0.7060–0.7061, 0.7036–0.7051, 0.7030–0.7032, 0.7050–0.7053, 0.7048–0.7056, respectively; Xu et al., 2003a, 2007, in press and unpublished). In contrast, the extrusive carbonatites show relatively high Cu, Ni and Ir abundances. Sample LX-2 has relatively high PGE (specially Ir, Ru and Rh) contents and little fractionation between Pt and Ir. The sample is richer in silica ($SiO_2 = 11.02\%$) than LX-1 ($SiO_2 = 2.67\%$; Xu et al., unpublished). The latter in general has a similar PGE concentration and distribution pattern to the intrusive carbonatites.

5. Discussion

All the carbonatites collected in this study are characterized by quite low concentrations of PGEs. This is surely a consequence of the very poor affinity of PGEs for carbonates. PGEs are inferred to be compatible in sulfides and experimentally determined Ni–Cu sulfide melt /silicate melt partition coefficients (Ds) for PGEs are on the order of 10^4 (Peach et al., 1990; Fleet et al., 1991, Peach et al., 1994, Fleet et al., 1996; Bezmen et al., 1994). Petrographic observations indicate that sulfide modal abundance is <1% in all the samples except for the MY (Table 1). The low content of sulfides can be caused by their removal during the alteration (Chazey and Neal,

Table 3
Nickel, copper (ppm) and platinum group element (ppb) contents of the intrusive and extrusive carbonatites

Samples	DLX-4	DLX-5	DLX-6	DLX-29	MNP-1	MNP-3	MNP-4	MNP-4*	MNP-5	MNP-6	MNP-18	MY-1	MY-2	MY-12	MY-15
	IC	IC	IC	IC	IC	IC	IC	IC	IC	IC	IC	IC	IC	IC	IC
Ni	2.61	0.684	bdl	bdl	8.14	7.84	8.85	8.85	9.47	9.44	7.65	28.2	18.3	9.80	6.86
Ir	bdl	0.003	0.004	0.014	bdl	bdl	bdl	bdl	bdl	0.004	bdl	0.014	0.015	0.007	0.002
Ru	0.013	0.015	0.008	0.009	0.013	0.011	0.023	0.028	0.009	0.011	0.009	0.029	0.031	0.033	0.026
Rh	0.011	0.010	0.004	0.01	bdl	0.003	bdl	bdl	0.003	0.011	0.031	0.014	0.020	0.003	bdl
Pt	0.357	0.385	0.180	0.188	0.401	0.569	0.539	0.607	1.350	0.996	0.885	0.127	0.216	0.054	0.015
Pd	0.214	0.253	0.164	0.128	0.675	0.154	0.237	0.250	0.407	0.529	0.339	0.702	0.984	0.306	0.063
Cu	15.1	9.12	bdl	2.33	bdl	0.87	7.84	7.84	0.116	0.511	bdl	19.0	11.1	8.10	1.71

| Samples	MY-16	MY-17	SDX-1	SXD-3	SXD-4	SXD-5	SXD-8	HYC-10	HYC-14	HYC-35	HYC-35*	HLP-1	HLP-2	HLP-3	LX-1	LX-1*	LX-2
	IC	IC	IC	IC	IC	IC	IC	IC	IC	IC	IC	IC	IC	IC	EC	EC	EC
Ni	8.01	12.1	bdl	bdl	0.023	5.70	4.13	0.663	bdl	bdl	Bdl	9.41	18.1	7.27	59.3	59.3	260
Ir	0.002	0.004	0.005	0.003	0.004	bdl	0.004	0.002	0.008	0.003	Bdl	bdl	0.002	bdl	0.024	0.027	0.194
Ru	0.008	0.023	0.031	0.053	0.011	0.037	0.071	0.030	0.035	0.028	0.032	0.047	0.005	0.008	0.020	0.022	0.278
Rh	bdl	bdl	0.001	0.014	0.004	0.007	0.006	0.010	0.005	bdl	0.012	0.007	0.003	0.018	0.014	0.015	0.107
Pt	0.030	0.028	0.011	0.142	0.031	0.063	0.090	0.091	bdl	0.034	0.070	0.184	0.090	0.150	0.231	0.289	0.470
Pd	0.034	0.038	0.180	0.523	0.097	0.302	0.568	0.245	0.029	0.056	0.028	0.089	0.069	0.318	0.436	0.546	1.450
Cu	1.70	12.8	5.73	1.98	3.75	15.5	8.06	bdl	bdl	bdl	bdl	1.03	8.08	14.8	11.7	11.7	38.3

DLX, Daluxiang, MNP, Maoniuping, MY, Miaoya, SXD, Shaxiongdong, HYC, Huayangchuan, HLP, Huanglongpu, LX, Lixian; * replicate PGE analyses of the same sample; bdl, below detection limit; IC = intrusive carbonatite; EX = extrusive carbonatite.

2005). Alternatively, the carbonatites reached sulfur saturation and the resulting immiscible sulfide melt was effectively removed. All carbonatites, except for the LX and MY samples, have narrow ranges of $\delta^{13}C$ (−5.94 to −8.24, −6.6 to −7.0, −5.7 to −6.1, −6.8 to 7.0, −5.5 to −6.9‰) and $\delta^{18}O$ values (7.6–8.6, 6.4–7.4, 6.9–8.1, 7.6–8.4, 8.7–10.9‰ for DLX, MNP, SXD, HYC and HLP, respectively; Xu et al., 2003a, 2007, in press and unpublished). These values suggest a primary magmatic, mantle-derived origin for the carbonatites (Keller and Hoefs, 1995), i.e. unaffected by superficial secondary processes (Fig. 4). The $\delta^{13}C$ and $\delta^{18}O$ isotopes of MY carbonatites, ranging from −2.9 to −6.7‰ and 9.5 to 13.2‰ (Xu et al., unpublished), are outside the 'primary carbonatite field' and show consistent enrichment. This may indicate sedimentary contamination or high temperature fractionation as modeled by Demény et al. (1998). Continental material typically has high concentration of sulfur (Wedepohl, 1995), and assimilation of such material may increase sulfur in the magmas. This may explain why MY carbonatites containing relatively high sulfides. However, they do not show higher PGE contents than other carbonatites, suggesting that PGEs in the carbonatites are not affected by enrichment of sulfur via wall-rock assimilation.

It is well accepted that carbonatite magmas are generated by extremely low degrees of partial melting ($F < 1\%$) of a carbonated peridotitic or eclogitic source (Nelson et al., 1988). The melts derived by small degree partial melting of primitive mantle are more likely to be S-saturated (Mitchell and Keays, 1981; Hamlyn et al., 1985; Zhou et al., 1998). As discussed by Keays and Lightfoot (2007), the low PGE concentrations together with low Pd/Cu ratios are the excellent hallmarks of S-saturated magmas, and the Pd/Cu ratios can be used to indicate S-saturation of magmas undergoing fractionation. Many carbonatites have low Pd/Cu ratios less than 1×10^{-4} (Table 3). Although the Ds between sulfide melt and carbonatite melt for PGEs are unknown, they are surely high (possibly greater than 1×10^4). Segregation of an immiscible sulfide melt may lead to the loss of PGEs in the carbonatites. Many low degrees of melting derived basalts from the continental sector of the Cameroon Line, West Africa, and the Atlantic and Indian Ocean, determined by Rehkämper et al. (1999) and Bézos et al. (2005), also show similar PGE contents (ranging from 0.11 to 2.17 ppb, 0.04 to 2.55 ppb, respectively) to the intrusive and extrusive carbonatites. They suggested that sulfide segregation played an important role in controlling the PGE concentrations in these basalts.

Notably, the intrusive and silicate-poor extrusive (LX-1) carbonatites have relatively low PGE (specially Ir, Ru and Rh) contents and fractionation of Pt and Ir. These features are distinct from the silicate-rich extrusive sample LX-2 (Fig. 3). This difference possibly reflects a common factor because the former in general has similar total PGE contents and distribution patterns. Table 1 shows that the silicate-rich extrusive carbonatite contains relatively abundant titanomagnetite and clinopyroxene. Experimental and petrological studies indicate that IPGEs (Ir and Ru) are more compatible in magnetite and pyroxene than PPGEs (Pt and Pd) (Capobianco et al., 1994; Puchtel and Humayun, 2001; Righter et al., 2004). Fractional crystallization of these mineral phases can result in the loss of IPGEs and positive primary mantle-normalized PGE patterns. In addition, because Cu is much less chalcophile than Pd (Ds for Cu and Pd in sulfide melt/silicate melt are ~700 and ~35 000, respectively; Peach et al., 1990), Cu-rich sulfide fractionation can result in low and variable Pd/Cu ratios. However, some intrusive and silicate-poor extrusive carbonatites show relatively high Pd/Cu and $(Pt/Ir)_n$ ratios (Fig. 5). Experiment shows that Cu is more soluble than other metals in volatile-rich fluids (Ballhaus et al., 1994). Therefore, the relatively high Pd/Cu ratios in these carbonatites may be due to segregation and loss of volatile-rich fluids.

Most chemical analyses of carbonatites do not represent the compositions of their melts. However, we suggest that the silicate-rich sample, LX-2, may approximate a carbonatite melt composition because (1) it contains relatively high PGE contents and unfractionated relative abundances; (2) it is extrusive. Fig. 6 shows that the sample LX-2 is strongly enriched in light rare earth elements (LREEs), but has lower total REE contents than intrusive carbonatites. Woolley et al. (1991) also found that extrusive carbonatites generally had lower contents of incompatible elements than intrusive ones. Ionov and Harmer (2002) suggested that relatively low REE abundances may be common in mantle-derived carbonate liquids, and enrichments in highly incompatible elements in many carbonatites may require fractionation of liquids during ascent. The above study also shows that the intrusive carbonatites may experience marked fractionation of sulfides, mafic silicates, oxides and volatile-rich fluids. In addition, Ds of REEs between melt and carbonate mineral are much less than 1 (Bühn et al., 2001). Re-crystallization and accumulation of carbonate minerals from a fractionated, late-stage melt should cause an increase in abundances of REEs and many other lithophile elements in most
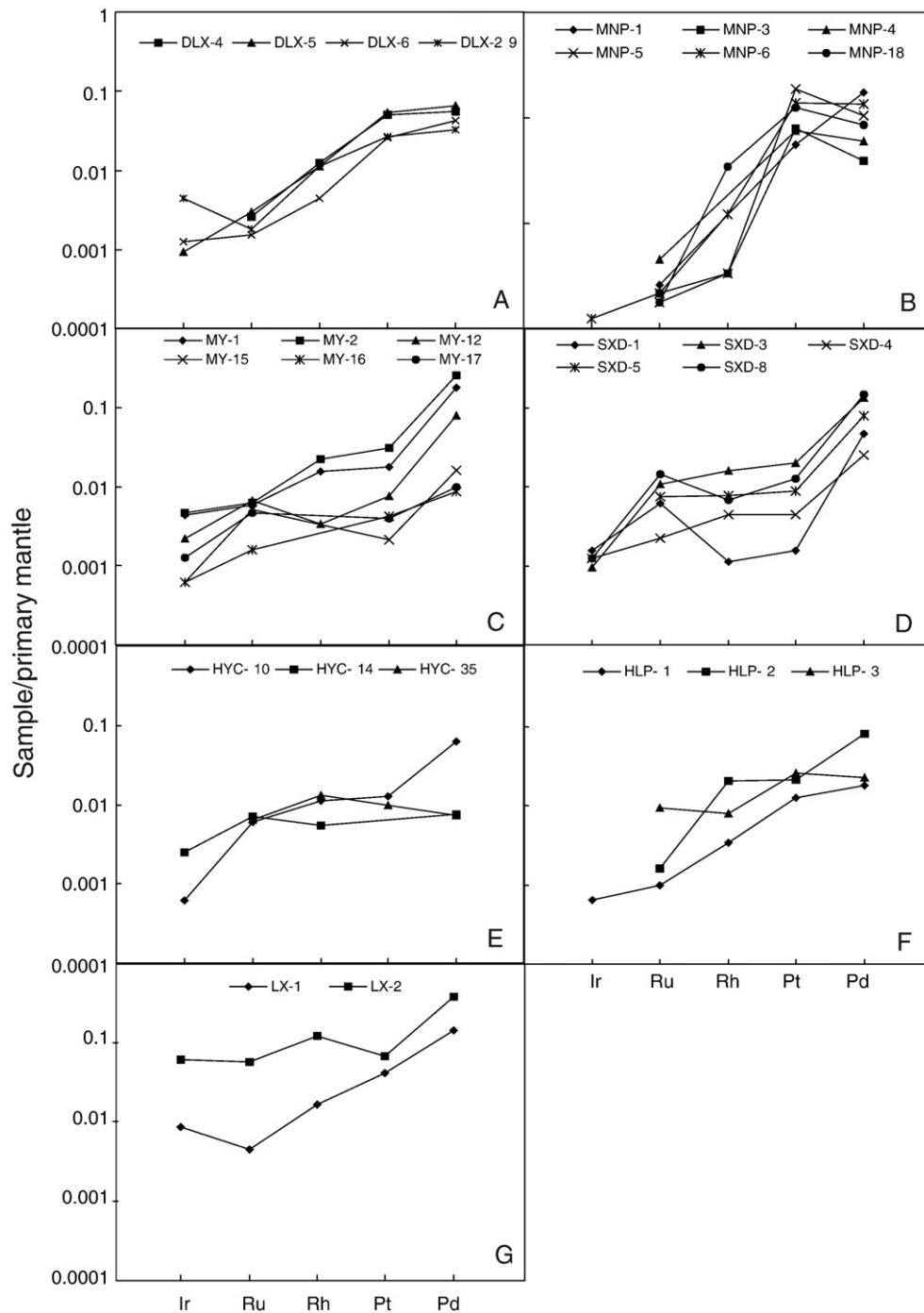
Fig. 3. Primary mantle-normalized PGE concentrations of carbonatites. A, Daluxiang; B, Maoniuping; C, Miaoya; D, Shaxiongdong; E, Huayangchuan; F, Huanglongpu; G, Lixian. Normalization values are from McDonough and Sun (1995).

intrusive carbonatites and corresponding carbonate minerals (e.g. Hornig-Kjarsgaard, 1998; Xu et al., 2007); (3) extrusive carbonatites are characterized by the very rapid rise of a turbulent mixture of solid, liquid and gas components enabling dense mantle material to be transported to the surface. However, intrusive carbonatites are likely to have been emplaced relatively passively, and involve one or more stages of ponding and differentiation of the magmas within the mantle or crust, or both, before final emplacement (Woolley and Church, 2005). The presence of abundant lapilli and clinopyroxene in the sample LX-2 demonstrates that the high PGE contents may represent mantle material entrained by the rising carbonatite magma.

6 . Conclusions

All carbonatites in this study contain low abundances of magmatic sulfides. Their magmas may reach sulfur saturation, and segregation of magmatic sulfides resulted in significant loss of PGEs in the carbonatites. The silicate-rich extrusive carbonatite has higher PGE (specially IPGE) contents and less fractionation between Pt and Ir than the intrusive and silicate-poor extrusive ones. It also has relatively abundant clinopyroxene and titanomagnetite. These features indicate that the intrusive and silicate-poor extrusive carbonatites may have experienced significant fractionation of sulfides and
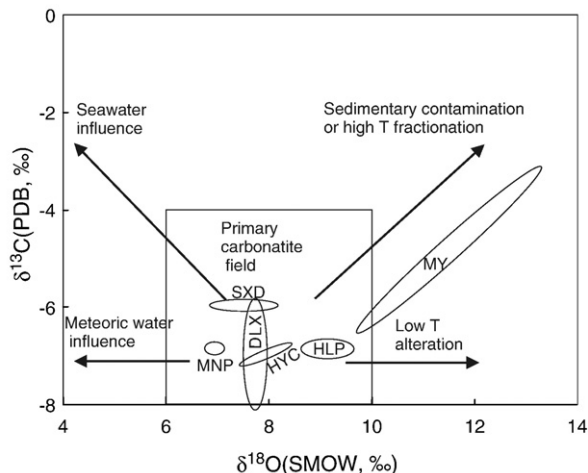
Fig. 4. Carbon and oxygen isotopic compositions of carbonatites, together with the field of primary, unaltered carbonatites of Keller and Hoefs (1995). Arrows indicate schematically the main processes responsible for changes in the C–O isotopic compositions (Demény et al., 1998). The data for Daluxiang (DLX), Maoniuping (MNP), Miaoya (MY), Shaxiongdong (SXD), Huayangchuan (HYC) and Huanglongpu (HLP) carbonatites are from Xu et al. (2003a, 2007, in press and unpublished).
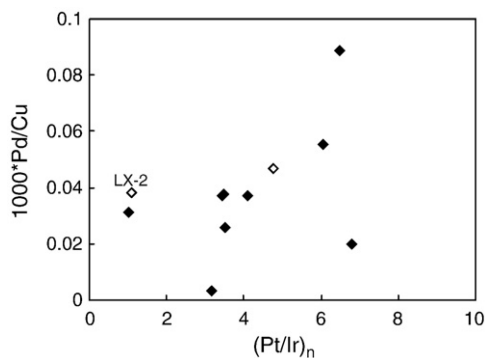

Fig. 6. Chondrite-normalized REE abundances of carbonatites. Data for the intrusive and extrusive are from Xu et al. (2003a, 2007, in press and unpublished). Normalization values are from McDonough and Sun (1995).

IPGE-rich mafic silicates and oxides during ascent or emplacement of magmas.

Acknowledgments

References

Bailey, D.K., 1993. Carbonatite magmas. Journal of the Geological Society (London) 150, 637–651.

Ballhaus, C., Ryan, C.G., Mernagh, T.P., Green, D.H., 1994. The partitioning of Fe, Ni, Cu, Pt, and Au between sulfide, metal, and fluid phases: a pilot study. Geochimica et Cosmochimica Acta 58, 811–826.

Bell, K., 1989. Carbonatites: Genesis and Evolution. Unwin Hyman, London.

Bell, K., Blenkinsop, J., 1987. Nd and Sr isotopic composition of East African carbonatites: implications for mantle heterogeneity. Geology 15, 99–102.

Bell, K., Tilton, G.R., 2001. Nd, Pb, and Sr isotopic compositions of East African cabonatites: evidence for mantle mixing and plume inhomogeneity. Journal of Petrology 42, 1927–1945.

Bezmen, N.I., Asif, M., Brügmann, G.E., Romaneko, I.M., Naldrett, A.J., 1994. Distribution of Pd, Rh, Ru, Ir, Os, and Au between sulfide and silicate melts. Geochimica et Cosmochimica Acta 58, 1251–1260.

Bézos, A., Lorand, J.P., Humler, E., Gros, M., 2005. Platinum-group element systematics in Mid-Oceanic Ridge basaltic glasses from the Pacific, Atlantic, and Indian Oceans. Geochimica et Cosmochimica Acta 69, 2613–2627.

Büchl, A., Brügmann, G.E., Muenker, C., Hofmann, A.W., 2002. Melt percolation monitored by Os-isotopes and PGE abundances: a case study from the mantle section of the Troodos ophiolite. Earth and Planetary Science Letters 204, 385–402.

Bühn, B., Wall, F., Le Bas, M.J., 2001. Rare-earth element systematics of carbonatitc fluorapatites, and their significance for carbonatite magma evolution. Contributions to Mineralogy and Petrology 141, 572–591.

Capobianco, C.J., Hervig, R.L., Drake, M.J., 1994. Experiments on crystal/liquid partitioning of Ru, Rh and Pd for magnetite and hematite solid solutions crystallized from silicate melt. Chemical Geology 113, 23–43.

Chazey, W.J., Neal, C.R., 2005. Platinum-group element constraints on source composition and magma evolution of the Kerguelen Plateau using basalts from ODP Leg 183. Geochimica et Cosmochimica Acta 69, 4685–4701.

Demény, A., Ahijado, A., Casillas, R., Vennemann, T.W., 1998. Crustal contamination and fluid/rock interaction in the carbonatites of Fuerteventura Canary Islands, Spain: a C, O, H isotope study. Lithos 44, 101–115.

Fleet, M.E., Stone, W.E., Crocket, J.H., 1991. Partitioning of palladium, iridium, and platinum between sulfide liquid and basalt melt: effects of melt composition, concentration, and oxygen fugacity. Geochimica et Cosmochimica Acta 55, 2545–2554.

Fleet, M.E., Crocket, J.H., Stone, W.E., 1996. Partitioning of platinum-group elements (Os, Ir, Ru, Rh, Pt, Pd) and gold between sulfide liquid and basalt melt. Geochimica et Cosmochimica Acta 60, 2397–2412.

Hamlyn, P.R., Keays, R.R., Cameron, W.E., Crawford, A.J., Waldron, H.M., 1985. Precious metals in magnesian low-Ti lavas: implications for metallogenesis and sulfur saturation in primary magmas. Geochimica et Cosmochimica Acta 49, 1797–1811.

Hoernle, K., Tilton, G., Le Bas, M.J., Duggen, S., Garbe-Schonberg, D., 2002. Geochemistry of oceanic carbonatites compared with continental carbonatites: mantle recycling of oceanic crustal carbonate. Contributions to Mineralogy and Petrology 142, 520–542.

Hornig-Kjarsgaard, I., 1998. Rare earth elements in sövitic carbonatites and their mineral phases. Journal of Petrology 39, 2105–2121.

Hou, Z.Q., Tian, S.H., Yuan, Z.X., Xie, Y.L., Yin, S.P., Yi, L.S., Fei, H.C., Yang, Z.M., 2006. The Himalayan collision zone carbonatites in western Sichuan, SW China: petrogenesis, mantle source and tectonic implication. Earth and Planetary Science Letters 244, 234–250.

Huang, D.H., Wu, C.Y., Du, A.D., He, H.L., 1994. Re–Os isotope ages of molybdenum deposits in east Qinling and their significance. Mineral Deposits 13, 221–230 (in Chinese with English Abstract).

Ionov, D., Harmer, R.E., 2002. Trace element distribution on calcite–dolomite carbonatites from Spitskop: inferences for differentiation of carbonatite magmas and the origin of carbonates in mantle xenoliths. Earth and Planetary Science Letters 198, 495–510.

Ionov, D.A., Shirey, B.D., Weis, D., Brügmann, G., 2006. Os–Hf–Sr–Nd isotope and PGE systematics of spinel peridotite xenoliths from Tok, SE Siberian craton: Effects of pervasive metasomatism in shallow refractory mantle. Earth and Planetary Science Letters 241, 47–64.

Keays, R.R., Lightfoot, P.C., 2007. Siderophile and chalcophile metal variations in Tertiary picrites and basalts from West Greenland with implications for the sulphide saturation history of continental flood basalt magmas. Mineralium Deposita 42, 319–336.

Keller, J., Hoefs, J., 1995. Stable isotope characteristics of recent natrocarbonatites from Oldoinyo Lengai. In: Bell, K., Keller, J. (Eds.), Carbonatites Volcanism: Oldoinyo

Fig. 5. $1000 \times Pd/Cu$ vs. $(Pt/Ir)_n$ diagram. ♦ = intrusive carbonatite; ◊ = extrusive carbonatite; n=normalized by primary mantle.

Lengai and Petrogenesis of Natrocarbonatites. LAVCEI Proceeding in Volcanology. Springer-Verlag, Berlin, pp. 113–123.

Liang, Q., Hu, J., Gregoire, D.C., 2000. Determination of trace elements in granites by inductively coupled plasma mass spectrometry. Talanta 51, 507–513.

McDonough, W.F., Sun, S.S., 1995. The composition of the Earth. Chemical Geology 120, 223–253.

Meisel, T., Fellner, N., Moser, J., 2003. A simple procedure for the determination of platinum group elements and rhenium (Ru, Rh, Pd, Re, Os, Ir and Pt) using ID-ICP-MS with an inexpensive on-line matrix separation in geological and environmental materials. Journal of Analytical Atomic Spectrometry 18, 720–726.

Meng, Q.R., Zhang, G.W., 2000. Geologic framework and tectonic evolution of the Qinling orogen, central China. Tectonophysics 323, 183–196.

Mitchell, R.H., Keays, R.R., 1981. Abundance and distribution of gold, palladium and iridium in some spinel and garnet lherzolites—implications for the nature and origin of precious metal-rich intergranular components in the upper mantle. Geochimica et Cosmochimica Acta 45, 2425–2442.

Momme, P., Tegner, C., Brooks, C.K., Keays, R.D., 2006. Two melting regimes during Paleogene flood basalt generation in East Greenland: combined REE and PGE modeling. Contributions to Mineralogy and Petrology 151, 88–100.

Nelson, D.R., Chivas, A.R., Chappell, B.W., McCulloch, M.T., 1988. Geochemical and isotopic systematics in carbonatites and implications for the evolution of ocean–island sources. Geochimica et Cosmochimica Acta 52, 1–17.

Peach, C.L., Mathez, E.A., Keays, R.R., 1990. Sulfide melt–silicate melt distribution coefficients for noble metals and other chalcophile elements as deduced from MORB: Implications for partial-melting. Geochimica et Cosmochimica Acta 54, 3379–3399.

Peach, C.L., Mathez, E.A., Keays, R.R., Reeves, S.J., 1994. Experimentally determined sulfide melt–silicate melt partition coefficients for iridium and palladium. Chemical Geology 117, 361–377.

Pu, G.P., 2001. The evolution history of REE mineralization and major features of Himalayan REE deposit in Panzhihua–Xichang area, Sichuan. In: Chen, Y.C., Wang, D.H. (Eds.), Study on Himalayan Endognic Mineralization. Geological Publishing House, Beijing, pp. 104–116 (in Chinese).

Puchtel, I.S., Humayun, M., 2001. Platinum group element fractionation in a komatitic basalt lava lake. Geochimica et Cosmochimica Acta 65, 2979–2993.

Qi, L., Zhou, M.F., Wang, C.Y., 2004. Determination of low concentrations of platinum group elements in geological samples by ID-ICP-MS. Journal of Analytical Atomic Spectrometry 19, 1335–1339.

Qi, L., Zhou, M.F., Wang, C.Y., Sun, M., 2007. Evaluation of a technique for determining Re and PGEs in geological samples by ICP-MS coupled with a modified Carius tube digestion. Geochemical Journal 41, 407–414.

Rehkämper, M., Halliday, A.N., Fitton, J.G., Lee, D.C., Wieneke, M., Arndt, N.T., 1999. Ir, Ru, Pt, and Pd in basalts and komatiites: new constraints for the geochemical behavior of the platinum-group elements in the mantle. Geochimica et Cosmochimica Acta 63, 3915–3934.

Righter, K., Campbell, A.J., Humayun, M., Hervig, R.L., 2004. Partitioning of Ru, Rh, Pd, Re, Ir, and Au between Cr-bearing spinel, olivine, pyroxene and silicate melts. Geochimica et Cosmochimica Acta 68, 867–880.

Rudashevsky, N.S., Kertser, Y.L., Bulakh, A.G., Rudashevsky, V.N., 2001. Two type of PGE mineralization in carbonatite deposit. Journal of African Earth Sciences 32, 30–30.

Shirey, S.B., Walker, R.J., 1995. Carius tube digestion for low-blank rhenium–osmium analysis. Analytical Chemistry 67, 2141–2163.

Tappe, S., Foley, S.F., Stracke, A., Romer, R.L., Kjarsgaard, B.A., Heaman, L.M., Joyce, N., 2007. Craton reactivation on the Labrador Sea margins: $^{40}Ar/^{39}Ar$ age and Sr–Nd–Hf–Pb isotope constraints from alkaline and carbonatite intrusives. Earth and Planetary Science Letters 256, 433–454.

Wedepohl, K.H., 1995. The composition of the continental crust. Geochimica et Cosmochimica Acta 59, 1217–1232.

Woolley, A.R., Church, A.A., 2005. Extrusive carboantites: a brief review. Lithos 85, 1–14.

Woolley, A.R., Barr, M.W.C., Din, V.K., Jones, G.C., Wall, F., Williams, C.T., 1991. Extrusive carbonatites from the Uyaynah area, United Arab Emirates. Journal of Petrology 32, 1143–1167.

Xu, C., Huang, Z.L., Liu, C.Q., Qi, L., Li, W.B., 2003a. Geochemistry of carbonatites in Maoniuping REE deposit Sichuan Province, China. Science in China (D) 46, 246–256.

Xu, C., Huang, Z.L., Liu, C.Q., Qi, L., Li, W.B., 2003b. PGE geochemistry of carbonatites in Maoniuping REE deposits, Sichuan Province, China: preliminary study. Geochemical Journal 37, 391–399.

Xu, C., Campbell, I.H., Allen, C.M., Huang, Z.L., Qi, L., Zhang, H., Zhang, G.S., 2007. Flat rare earth element patterns as an indicator of cumulate processes in the Lesser Qinling carbonatites, China. Lithos 95, 267–278.

Xu, C., Campbell, I.H., Allen, C.M., Chen, Y.J., Huang, Z.L., Qi, L., Zhang, G.S., in press. U–Pb zircon age, geochemical and isotopic characteristics of carbonatite and syenite complexes from the Shaxiongdong, China. Lithos.

Xu, C., Kynicky, J., Campbell, I.H., Allen, C.M., Chen, Y.J., Huang, Z.L., Qi, L., unpublished. Comparison of the Daluxiang and Maoniuping carbonatitic REE deposits with Bayan Obo REE deposit, China.

Xu, C., Kynicky, J., Campbell, I.H., Allen, C.M., Chen, Y.J., unpublished. REE minerals and calcite from the Miaoya carbonatites, China: implications for REE mineralization.

Yin, A., Harrison, T.M., 2000. Geologic evolution of the Himalayan–Tibetan orogen. Annual Review of Earth and Planetary Sciences 28, 211–280.

Yu, X.H., 1992. Geological, mineralogical characteristics and origin of the carbonatites from Huayangchuan, Shanxi Province. Earth Science 17, 151–158 (in Chinese with English abstract).

Yu, X.H., Mo, X.X., Su, S.G., Dong, F.L., Zhao, X., Wang, C., 2003. Discovery and significance of Cenozoic volcanic carbaontite in Lixian, Gansu Province. Acta Petrologica Sinica 19, 105–112 (in Chinese with English Abstract).

Yu, X.H., Zhao, Z.D., Mo, X.X., Zhu, D.Q., Wang, Y.L., 2006. $^{40}Ar/^{39}Ar$ dating for Cenozoic kamafugite from western Qinling in Gansu Province. Chinese Science Bulletin 51, 1621–1627.

Zhou, M.F., Sun, M., Keays, R.R., Kerrich, R.W., 1998. Control on platinum-group elemental distributions of podiform chromitites: a case study of high-Cr and high-Al chromitites from Chinese orogenic blets. Geochimica et Cosmochimica Acta 62, 677–688.